THE JOURNAL OF BIOLOGICAL CHEMISTRY
Vol. 276, No. 26, Issue of June 29, pp. 24015–24022, 2001

Printed in U.S.A.

Structure and Mechanism of Action of an Indolicidin Peptide Derivative with Improved Activity against Gram-positive Bacteria*

Received for publication, October 23, 2000, and in revised form, April 2, 2001
Published, JBC Papers in Press, April 9, 2001, DOI 10.1074/jbc.M009691200

Carol L. Friedrich, Annett Rozek‡, Aleksander Patrzykat, and Robert E. W. Hancock§

From the Department of Microbiology and Immunology, University of British Columbia, Vancouver, British Columbia V6T 1Z3, Canada

Indolicidin, an antimicrobial peptide with a unique amino acid sequence (ILPWKWPWWPWRR-NH_2) is found in bovine neutrophils. A derivative of indolicidin, CP10A, has alanine residues substituted for proline residues and has improved activity against Gram-positive organisms. Transmission electron microscopy of *Staphylococcus aureus* and *Staphylococcus epidermidis* treated with CP10A showed mesosome-like structures in the cytoplasm. The peptide at 2-fold the minimal inhibitory concentration did not show significant killing of *S. aureus* ISP67 (a histidine, uridine, and thymidine auxotroph) but did show an early effect on histidine and uridine incorporation and, later, an effect on thymidine incorporation. Upon interaction with liposomes, detergents, and lipoteichoic acid, CP10A was shown by circular dichroism spectroscopy to undergo a change in secondary structure. Fluorescence spectroscopy indicated that the tryptophan residues were located at the hydrophobic/hydrophilic interface of liposomes and detergent micelles and were inaccessible to the aqueous quencher KI. The three-dimensional structure of CP10A in the lipid mimetic dodecylphosphocholine was determined using two-dimensional NMR methods and was characterized as a short, amphipathic helical structure, whereas indolicidin was previously shown to have an extended structure. These studies have introduced a cationic peptide with a unique structure and an ability to interact with membranes and to affect intracellular synthesis of proteins, RNA, and DNA.

Antimicrobial cationic peptides are ubiquitous in nature and are thought to be an important component in innate host defenses against infectious agents (1). There are four structural classes of cationic antimicrobial peptides; the disulfide-bonded β-sheet peptides, including the defensins; the amphipathic α-helical peptides such as the cecropins and melittins; the extended peptides, which often have a single amino acid predominating (*e.g.* indolicidin); and the loop-structured peptides like bactenecin (1). The initial interactions of some cationic peptides with Gram-negative bacteria are thought to involve binding to surface lipopolysaccharide (2, 3). The peptides displace divalent cations that are essential for outer membrane integrity and consequently distort the outer membrane bilayer (4). This allows access to the cytoplasmic membrane where peptide channel formation has been proposed to occur (5). It is increasingly disputed as to whether peptide channel formation leads to dissolution of the proton motive force and leakage of essential molecules (6, 7) or whether it is an intermediate step in the uptake of peptide into the cytoplasm, where it inhibits an essential function by *e.g.* binding to polyanionic DNA (8–10).

Indolicidin is a 13-amino acid cationic peptide present in the cytoplasmic granules of bovine neutrophils (11). Indolicidin has a unique amino acid composition (ILPWKWPWWPWRR-NH_2) with 39% tryptophan, 23% proline, and an amidated carboxyl terminus. This, along with the fact that it has a broad spectrum of antimicrobial activity, has made it an interesting candidate for study. The structure of indolicidin was determined by two-dimensional NMR and shown to form an extended boat-shaped conformation when bound to dodecylphosphocholine (DPC)[1] (12). Previous structure-function studies by Subbalakshmi *et al.* (13) led to the design of a peptide ILA, called here CP10A. CP10A is a peptide with the three proline residues of indolicidin replaced with alanine, resulting in the amino acid sequence ILAWKWAWWAWRR-NH_2. Subbalakshmi *et al.* (13) found that these amino acid substitutions had no effect on the activity against *Escherichia coli* and *Staphylococcus aureus* (13). However, our previous studies show that CP10A has 2–8-fold better activity against most Gram-positive bacteria (14). In the present work we examined the structure and the mode of action of CP10A against Gram-positive bacteria in greater detail using a variety of biophysical and biochemical methods.

Various studies of the effects of cationic peptides on the membranes of Gram-positive bacteria have been conducted. Previous studies of peptide effects on membrane potential show that there are effects on the cytoplasmic membrane of *S. aureus* (14, 15). As well, ultrastructural studies of *S. aureus* treated with defensins (16) and platelet microbicidal proteins (15) showed cell membrane damage followed by cell death. The defensins caused mesosome-like structures to appear before the bacteria lost their viability, but no remarkable effects on the cell wall were seen (16). These studies suggested that membrane perturbation is an important, but not necessarily lethal, event. Recent studies indicate that some peptides may indeed have an intracellular target. Xiong *et al.* (17) find that *S.*

* This work was supported by grants from the Canadian Bacterial Diseases Network and the Canadian Cystic Fibriosis Foundation. The costs of publication of this article were defrayed in part by the payment of page charges. This article must therefore be hereby marked "*advertisement*" in accordance with 18 U.S.C. Section 1734 solely to indicate this fact.

‡ Holds a fellowship from the Canadian Institute of Health Research.
§ Holds a Distinguished Scientist Award from the Canadian Institute of Health Research. To whom correspondence should be addressed: Dept. of Microbiology and Immunology, University of British Columbia, 300-6174 University Blvd., Vancouver, British Columbia V6T 1Z3, Canada. Tel.: 604-822-2682; Fax: 604-822-6041; E-mail: bob@cmdr.ubc.ca.

[1] The abbreviations used are: DPC, dodecylphosphocholine; POPC, 1-palmitoyl-2-oleoyl-*sn*-glycero-3-phosphocholine; POPG, 1-palmitoyl-2-oleoyl-*sn*-glycero-3-phosphoglycerol; head group labeled tempo-PC, 1,2-dioleoyl-*sn*-glycero-3-phosphotempocholine; 5-doxyl-PC, 1-palmitoyl-2-stearoyl-(5-doxyl)-*sn*-glycero-3-phosphocholine; 12-doxyl-PC, 1-palmitoyl-2-stearoyl-(12-doxyl)-*sn*-glycero-3-phosphocholine; MIC, minimal inhibitory concentration; CD, circular dichroism; TOCSY, total correlation spectroscopy; NOESY, nuclear Overhauser effect (/enhancement) spectroscopy; DQF-COSY, double quantum-filtered correlation spectroscopy.

aureus, pretreated with inhibitors of DNA gyrase or protein synthesis, demonstrated decreased or blocked killing by human neutrophil peptide-1 and platelet microbicidal protein-1, whereas pretreatment with bacterial cell wall synthesis inhibitors enhanced bacterial killing. The authors concluded that these cytoplasmic membrane effects occurred before effects on protein and DNA synthesis. As well, in our lab we demonstrated a lack of correlation between bacterial killing and cytoplasmic membrane depolarization and, in *Staphylococcus epidermidis*, nuclear condensation, indicating effects on DNA (14). There is thus growing evidence for an intracellular target for some antimicrobial cationic peptides. Here we describe a peptide with a unique structure that causes ultrastructural effects on *S. aureus* and *S. epidermidis* similar to those seen with other cationic peptides as well as intracellular effects.

EXPERIMENTAL PROCEDURES

Materials and Bacterial Strains—CP10A (ILAWKWAWWAWRR-NH_2) was synthesized by Fmoc (*N*-(9-fluorenyl)methoxycarbonyl) chemistry at the Nucleic Acid Protein Service (NAPS) unit at the University of British Columbia. The peptide was pure, as confirmed by high performance liquid chromatography and mass spectrometry. Bovine serum albumin fraction V lyophilizate was purchased from Roche Molecular Biochemicals. *S. aureus* ATCC 25923, and *S. epidermidis* (clinical isolate, obtained from David Speert, University of British Columbia) (18) were used for electron microscopy. *S. aureus* ISP67 (obtained from John Iandolo, Kansas State University), a strain auxotrophic for thymidine, uridine, and histidine, was used in the macromolecular synthesis studies. In most cases Luria-Bertani media (no salt) (Difco) was used as a growth medium, with the exception of *S. aureus* ISP67, which was grown in modified complete synthetic media (salts, glucose, amino acids, Lindberg vitamins, niacin, and thiamine) supplemented with 20 mg/liter thymidine, 5 mg/liter uridine, and 20 mg/liter histidine (Sigma). Dipropylthiacarbocyanine (5) was purchased from Molecular Probes (Eugene, OR). Perdeuterated DPC (DPC-d_{38}) and deuterium oxide (D_2O) were purchased from Cambridge Isotope Laboratories, Andover, MA. 1-Palmitoyl-2-oleoyl-*sn*-glycero-3-phosphocholine (POPC) and 1-palmitoyl-2-oleoyl-*sn*-glycero-3-phosphoglycerol (POPG) were purchased from Northern Lipids Inc., Vancouver, BC, Canada. 1,2-Dioleoyl-*sn*-glycero-3-phosphotempocholine (head group labeled tempo-PC), 1-palmitoyl-2-stearoyl-(5-doxyl)-*sn*-glycero-3-phosphocholine (5-doxyl-PC), and 1-palmitoyl-2-stearoyl-(12-doxyl)-*sn*-glycero-3-phosphocholine (12-doxyl-PC) were obtained from Avanti Polar Lipids Inc., Alabaster, AL.

Transmission Electron Microscopy—Exponential phase bacteria were treated with the peptide at 10 times the minimal inhibitory concentration (MIC) for 10 min at 37 °C. This concentration was used to see an effect on a greater fraction of cells. After treatment, the bacterial pellets were fixed with 2.5% buffered glutaraldehyde for 1 h. The cells were then post-fixed in 1% buffered osmium tetroxide for 1 h, stained en bloc with 1% uranyl acetate, dehydrated in a graded series of ethanol, and embedded in Spur resin. The buffer used was 0.1 M sodium cacodylate (pH 7.4). Thin sections were prepared on Formvar copper grids and stained with 2% uranyl acetate and lead citrate. The resin and grids were purchased from Canemco (Toronto, ON, Canada). Microscopy was performed with a Zeiss Stem 10C microscope under standard operating conditions.

Minimal Inhibitory Concentration—The MIC of CP10A was determined using a broth microdilution assay modified from the method of Amsterdam (19). Briefly, serial dilutions of the peptide were made in 0.2% bovine serum albumin, 0.01% acetic acid solution in 96-well polypropylene (Costar, Corning Inc., Corning, NY) microtiter plates. Each well was inoculated with 100 μl of the test organism in Luria-Bertani (no salt) broth or in the synthetic media to a final concentration of $\sim 10^5$ colony-forming units/ml. The MIC was taken as the lowest peptide concentration at which growth was inhibited after 24 h of incubation at 37 °C.

Cytoplasmic Membrane Depolarization Assay—The depolarization of the cytoplasmic membrane of *S. aureus* by the peptides was determined using the membrane potential-sensitive cyanine dye dipropylthiacarbocyanine (5) (20) by a modification of the method of Wu *et al.* (8), as described in Friedrich *et al.* (14).

Macromolecular Synthesis and Bacterial Killing Assays—Overnight cultures of *S. aureus* ISP67 were diluted 100-fold in synthetic media and allowed to grow to exponential phase (optical density at 600 nm of 0.3). The cultures were spun down and resuspended in warm synthetic media with 20 mg/liter [^{3}H]thymidine, 5 mg/liter [^{3}H]uridine, or 20 mg/liter [^{3}H]histidine. After 5 min of incubation at 37 °C, CP10A was added at 2- and 10-fold its MIC. Samples (50 μl) were removed at 0 min (before peptide) and 5, 10, 20, and 40 min and added to cold 5% trichloroacetic acid (purchased from Fisher Scientific) with excess unlabeled precursors to precipitate the macromolecules. After 40 min on ice and 15 min at 37 °C, the samples were collected over a vacuum on Whatman 47 mm GF/C glass microfibre filters (VWR Canlab, Mississauga, ON, Canada) and washed with cold trichloroacetic acid. The filters were collected and put into scintillation vials with ReadySafe liquid scintillation mixture (Beckman Instruments) and counted on a scintillation counter to measure precursor incorporation into macromolecules. At the same time points, 5-μl samples were removed from nonradioactive parallel cultures, diluted in 1 ml of buffer, and plated on to LB plates with added supplements to obtain a viable count.

Preparation of Liposomes—A chloroform solution of lipid was mixed with the peptide dissolved in methanol. This solution was dried under a stream of N_2 in vacuum to remove the solvent. The resulting lipid/peptide film was rehydrated in 10 mM phosphate buffer (pH 7.0). The suspension was put through five cycles of freeze-thaw to produce multilamellar liposomes, followed by extrusion through a 0.1-μm double-stacked Poretics filters (AMD Manufacturing Inc., Mississauga, ON, Canada) using an extruder device (Lipex Biomembranes, Vancouver, BC, Canada).

Fluorescence Spectroscopy—Fluorescence emission spectra were recorded on an LS 50B spectrofluorimeter (PerkinElmer Life Sciences). Measurements were performed between 300 and 450 nm at 1-nm increments using a 5-mm quartz cell at room temperature. The excitation wavelength was set to 280 nm with both the excitation and emission slit widths set to 4 nm. Spectra were base-line-corrected by subtracting blank spectra of the corresponding lipid or detergent solutions without peptide. The samples contained 2 μM peptide and 0.5 mM lipid or 10 mM detergent in 10 mM HEPES buffer (pH 7.2). The aqueous quencher potassium iodide was added in increasing increments to assess tryptophan accessibility to the aqueous buffer. Spin labeled lipids were used to estimate the tryptophan position in the liposomes.

Circular Dichroism Measurements—Circular Dichroism (CD) spectra were obtained using a J-720 spectropolarimeter (Japan Spectroscopic Co., Tokyo, Japan). Each spectrum (190–250 nm) was the average of 4 scans using a quartz cell of 1-mm path length at room temperature. The scanning speed was 50 nm/min at a step size of 0.1 nm, 2 s response time and 1.0-nm bandwidth. All samples were 50 μM peptides in 10 mM sodium phosphate buffer (pH 7.0). The concentrations of lipid or detergent were 2 or 10 mM, respectively. Spectra were base-line-corrected by subtracting a blank spectrum of a sample containing all components except the peptide. After noise correction, ellipticities were converted to mean residue molar ellipticities [θ] in units of deg $\times$ cm^2/dmol.

Nuclear Magnetic Resonance (NMR) Spectroscopy—The sample of CP10A was prepared by adding a solution of perdeuterated DPC in 10 mM sodium phosphate buffer (pH 5) containing 10% D_2O to the lyophilized peptide to give concentrations of 2 mM CP10A and 200 mM DPC-d_{38}. The pH was adjusted to 4.0 (uncorrected for the isotope effect). NMR spectra were recorded at 37 and 42 °C on a Bruker AMX600 spectrometer operating at 600.13 MHz. Homonuclear TOCSY (21), NOESY (22), and DQF-COSY (23) spectra were acquired. Water suppression was achieved using the WATERGATE technique (24, 25) or by presaturation during the recycling delay (2–2.5 s). Spectra were collected with 512–800 data points in F1, 2000 data points F2, and 32–64 transients. TOCSY spectra were acquired using the Malcolm Levitt (MLEV)-17 pulse sequence (26) at a spin-lock time of 80 ms. NOESY spectra were recorded at mixing times of 70, 100, and 150 ms.

Qualitative exchange rates of labile hydrogen atoms of CP10A in DPC micelles at 37 °C were determined by dissolving the lyophilized peptide in D_2O containing DPC-d_{38} at a molar ratio of peptide to detergent of 1:100. The pH* was determined to be 3.9 (uncorrected for the isotope effect). Several one-dimensional NMR spectra were acquired during the first hour after dissolution in D_2O. Then a TOCSY spectrum with a total acquisition time of $\sim$5 h was recorded followed by another one-dimensional spectrum to detect any slowly exchanging protons.

The NMR data were processed with NMRPIPE (27). Resolution enhancement was achieved by apodization of the free induction decay with shifted squared sine-bell window functions. The data were zero-filled to at least twice the size before Fourier transformation. Spectra were base-line-corrected using a 5th order polynomial function. All chemical shifts were referenced to internal 4,4-dimethyl-4-silapentane-1 sulfonate (DSS).

NOE Data Analysis and Structure Calculation—All NMR spectra

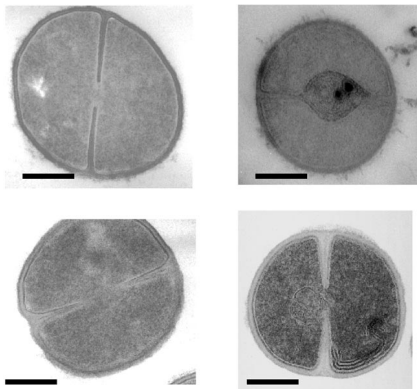

FIG. 1. **Electron micrographs of *S. aureus* control (*top left*) and CP10A-treated (*top right*) and *S. epidermidis* control (*bottom left*) and CP10A-treated (*bottom right*).** CP10A was at a concentration of 10-fold the MIC. The *bar* represents 250 nm.

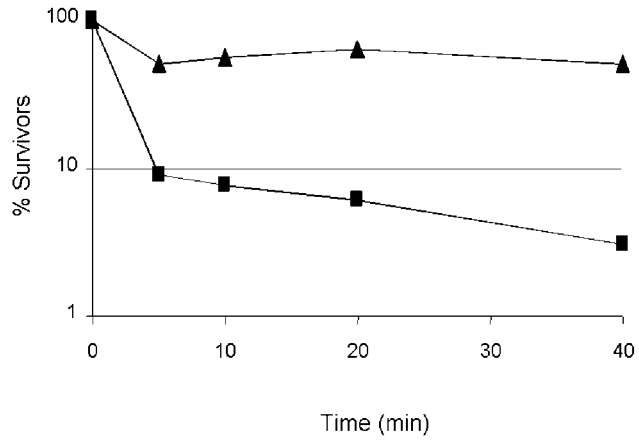

FIG. 2. **Percent survivors in the presence of 10-fold the MIC (*squares*) and 2-fold the MIC (*triangles*) of CP10A under conditions identical to the macromolecular synthesis assay.** No cell death occurred in the absence of peptide.

were analyzed using NMRVIEW version 4.0.5 (28). NOE cross-peaks were integrated in the NOESY spectra acquired at 37 °C using a mixing time of 70 ms. The NOE volumes were converted to distances, which were calibrated using the average NOE volume of all resolved geminal methylene proton cross-peaks as well as cross-peaks between tryptophan aromatic ring protons. The H^N-H^α distances thus calculated ranged from 2.65 to 2.99 Å, which is well within the covalently restricted range (2.3–3.1 Å). Each distance was converted to a distance restraint by calculating upper and lower distance bounds using the equations suggested by Hyberts *et al.* (29). Pseudo atom corrections were applied by adding 1 and 1.5 Å to the upper distance bound for unresolved methylene protons and methyl groups, respectively. Distance restraints involving resolved methylene protons were float-corrected by adding 1.7 Å to the upper bound. Structure calculations were performed using the distance geometry/simulated annealing programs DGII (Molecular Simulations Inc., San Diego, CA) and X-PLOR version 3.851 (30–32). Of 20 structures generated by DGII, 16 structures that had 3–6 NOE distance restraint violations of 0.1 Å were refined using X-PLOR and the CHARMM force field. The refinement consisted of simulated annealing, decreasing the temperature from 310 to 10 K over 50,000 steps (0.001 ps), resulting in 15 structures that converged with final energies of 25 ± 1 kcal/mol and 6 ± 1 NOE distance restraint violations ≥0.1 Å. The average largest NOE distance restraint violation was 0.20 ± 0.02 Å.

RESULTS

Transmission Electron Microscopy—Thin sections of CP10A-treated *S. epidermidis* and *S. aureus* were prepared to observe ultrastructural changes (Fig. 1). The bacteria were treated with 10-fold MIC of CP10A for 10 min before fixing (20 μg/ml and 40 μg/ml for *S. epidermidis* and *S. aureus*, respectively). These electron micrographs showed the formation of intracellular lamellar membranes (mesosomes) in peptide-treated cells only. Often these mesosomes occurred around the septum. In contrast to the indolicidin-related peptide CP11CN-treated *S. epidermidis* cells (14), no nuclear condensation was seen, and there appeared to be minimal cell wall effects with CP10A-treated cells. No apparent lysis or gross leakage of cellular cytoplasmic contents was observed.

Minimal Inhibitory Concentrations—We have previously shown (14) that CP10A had the same (*Streptococcus hemolyticus* and *Corynebacterium xerosis*) or 2–8-fold lower (*S. aureus*, methicillin-resistant *Staphylococcus aureus*, *S. epidermidis*, *Enterococcus faecalis*, *Listeria monocytogenes*, *Streptococcus pyogenes*) MICs compared with indolicidin against Gram-positive bacteria. For macromolecular synthesis studies, we determined the MICs of CP10A on the *S. aureus* wild-type strain (ATCC 25923) and the auxotrophic strain (ISP 67) in the presence of both LB and synthetic media. This was done to ensure that there are no significant differences between the two strains. The MIC of CP10A against the wild type was 2–4 μg/ml in LB and 2 μg/ml in the synthetic media. The MIC of CP10A against the auxotroph was 2 μg/ml in LB and 1 μg/ml in synthetic media. These results showed that there were no significant differences in activity against the two strains and in the two media.

Macromolecular Synthesis and Bacterial Killing Assays—To determine if CP10A had intracellular effects, we performed standard macromolecular synthesis assays. *S. aureus* ISP67 was used in macromolecular synthesis experiments in the presence of 2- and 10-fold the MIC of CP10A. Killing assays done in conjunction with these experiments (Fig. 2) showed that at 2-fold MIC there were 50% or more survivors over the first 40 min, whereas at 10-fold MIC, there were less than 10% survivors in the same time frame. Nonetheless, there was no significant difference between the two concentrations in macromolecular synthesis effects (Fig. 3), which demonstrated nearly complete inhibition. These results indicated that the effects on macromolecular synthesis at low peptide concentrations were probably not the result of dead or dying cells. Macromolecular synthesis of DNA, RNA, and proteins did not cease simultaneously, as expected if this was merely membrane disruption resulting in leakage of essential molecules. Histidine and uridine incorporation (Fig. 3, *B* and *C*) appeared to be affected first, with differences within the first 5 min after the peptide addition. Thymidine incorporation (Fig. 3*A*) was not affected until after 10 min. These results revealed that CP10A had intracellular effects on *S. aureus*.

Cytoplasmic Membrane Depolarization Assay—To determine if CP10A had the ability to depolarize the cytoplasmic membrane of *S. aureus*, we used the membrane potential-sensitive dye dipropylthiacarbocyanine (5). CP10A almost completely depolarized the membrane at a concentration of 1 μg/ml (data not shown) within 5 min. These results were similar to those found with the α-helical peptides CP26 and CP29, which completely depolarized the membrane at low concentrations (14). In contrast, indolicidin and its derivative CP11CN never completely depolarized the cytoplasmic membrane of either *S. aureus* (14) or *E. coli* (8).

Interaction with Detergents and Lipids; Fluorescence and CD Spectroscopy—The conformation of CP10A was determined using NMR spectroscopy in the presence of DPC; therefore, it was important to establish that the structure of this peptide formed upon binding to detergent micelles was similar to the structure when bound to phospholipid bilayers, which more closely resemble the bacterial cytoplasmic membrane. Fluorescence and CD spectroscopy are suitable methods for comparing the inter-

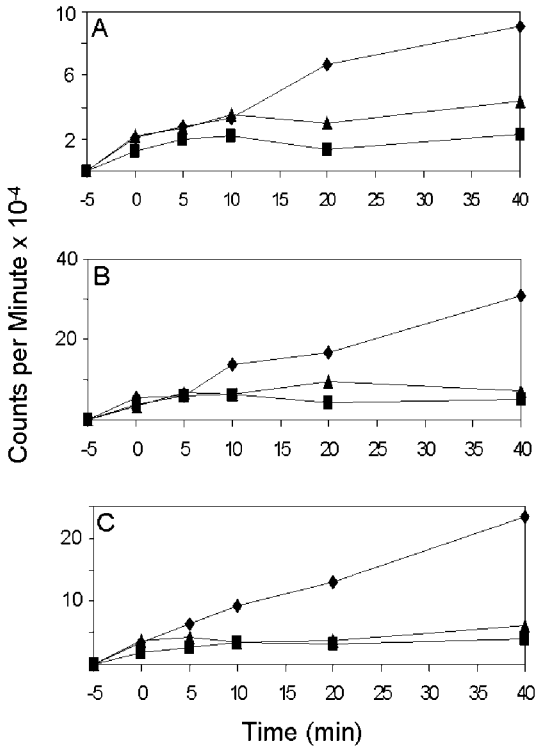

FIG. 3. **Effect of CP10A at 2-fold the MIC (*triangles*) and 10-fold the MIC (*squares*) on ^{3}H-labeled thymidine (*A*), uridine (*B*), and histidine (*C*) incorporation into *S. aureus* ISP67 DNA, RNA, and protein macromolecules.** *Diamonds*, control.

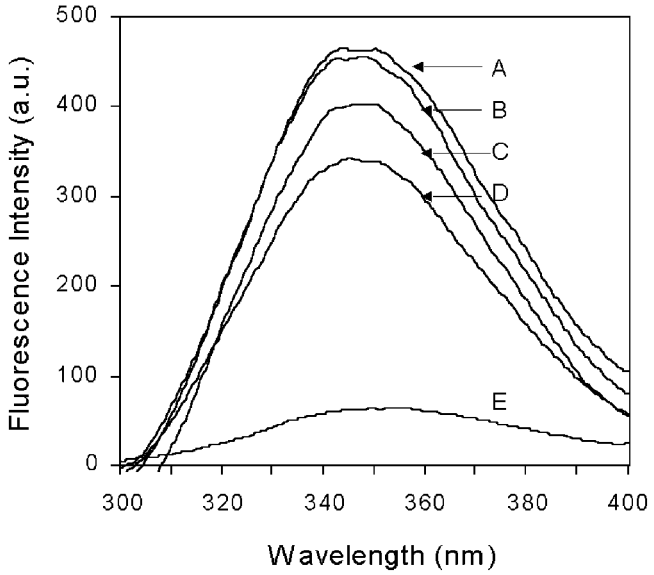

FIG. 4. **Fluorescence emission spectra of CP10A in complexes with DPC (*A*), POPC:POPG (7:3) liposomes (*B*), POPC liposomes (*C*), POPG liposomes (*D*), and buffer (*E*).** The samples contained 2 μM peptide and 0.5 mM lipid or 10 mM detergent in 10 mM HEPES buffer (pH 7.2). The emission maximum of CP10A was at 355 nm in buffer and 347 nm in complexes with DPC and liposomes. *a.u.*, arbitrary units.

action of peptides in different membrane environments. The fluorescence spectra of CP10A in aqueous solution and bound to different lipid and detergents are shown in Fig. 4. The emission maximum of the peptide in buffer alone was around 355 nm. With all lipid environments, an 8-nm blue shift of the emission maximum as well as an increase in fluorescence intensity occurred, indicating a transfer of the tryptophan side chains from an aqueous to a hydrophobic environment (33). The emission spectra in POPC, POPG, POPC:POPG (7:3), and DPC were all very similar, with peak wavelengths of around 347 nm, indicating that the environment experienced by the peptide in lipids and DPC was comparable. When the aqueous quencher KI was added in increments (data not shown), no change in fluorescence intensity was observed if the peptide was in the presence of liposomes, indicating that the tryptophan residues had become inaccessible to the aqueous buffer. Liposomes with incorporated spin-labeled lipids were used to estimate the average position of the tryptophan residues in the liposome, as spin labels will cause a decrease in tryptophan fluorescence when in close proximity. In the presence of head group labeled tempo-PC, there was an approximate 35% decrease in fluorescence. In the presence of 5-doxyl-PC and 12-doxyl-PC, there was ~45 and 48% decrease, respectively. The absence of a significant difference between the effects caused by 5-doxyl-PC and 12-doxyl-PC may be explained by the presence of five tryptophan residues in CP10A. Some of the tryptophan side chains may have resided near the 5-doxyl group, whereas others were near the 12-doxyl group. It is also possible that most of the tryptophan residues were located in an intermediate position between the 5- and 12-doxyl positions, resulting in similar effects for both spin labels. Similar results were found with the parent peptide indolicidin, which showed a 28% reduction in fluorescence intensity with head group-labeled tempo-PC and a 51% reduction for both 5- and 12-doxyl-PC (12). Hence, both indolicidin and CP10A resided in the bilayer interface, which is also the preferred location of tryptophan (43).

The CD spectra of free and lipid-bound CP10A are shown in Fig. 5*A*. The peptide, when bound to POPC, POPC:POPG (7:3), DPC (Fig. 5*A*), and lipoteichoic acid (data not shown), exhibited similar spectra with minima at around 207 and 218 nm as well as a maximum around 230 nm. There was also a maximum around 195 nm seen in the presence of DPC that could not be observed in the presence of liposomes due to interference by light scattering below 200 nm (34). The double minimum at 207 and 218 nm along with the maximum at 195 nm were indicative of α-helical structure (35). The maximum at 230 nm was likely due to the presence of tryptophan residues (36). The similarity of CD curves verified that the structure of CP10A in the presence of DPC is comparable with that seen in the presence of POPC and mixed liposomes. The CD spectrum of CP10A in POPG was different from the spectra in POPC, mixed liposomes, and DPC, indicating that binding of the peptide to POPG, as evidenced by the blue shift of the fluorescence spectrum, led to a different secondary structure. In aqueous solution and trifluoroethanol the CD bands at 207, 218, and 195 nm were also observed, albeit with reduced intensity, indicating that a helical structure is also present in the absence of lipids. However, the maximum at 230 nm was not present, suggesting a less defined tryptophan side chain orientation. These results indicated that CP10A formed a more ordered structure in the presence of lipids. The spectra of the parent peptide indolicidin are shown for comparison in Fig. 5*B*. Although CP10A was significantly α-helical in buffer, the spectrum of indolicidin in buffer was indicative of random coil, β-turn, or polyproline II helix (12).

NMR-derived Structure—The structure of CP10A was determined using proton nuclear magnetic resonance methods. Two-dimensional TOCSY, NOESY, and DQF-COSY spectra were acquired at 37 °C and pH 4.0. The proton resonances were completely assigned using the sequential assignment strategy (37). The chemical shifts are summarized in Table I. Fig. 6 presents a region of the NOESY spectrum showing the well resolved network of cross-peaks between the α-protons and backbone amide protons (7.5–8.8 ppm) as well as many inter-

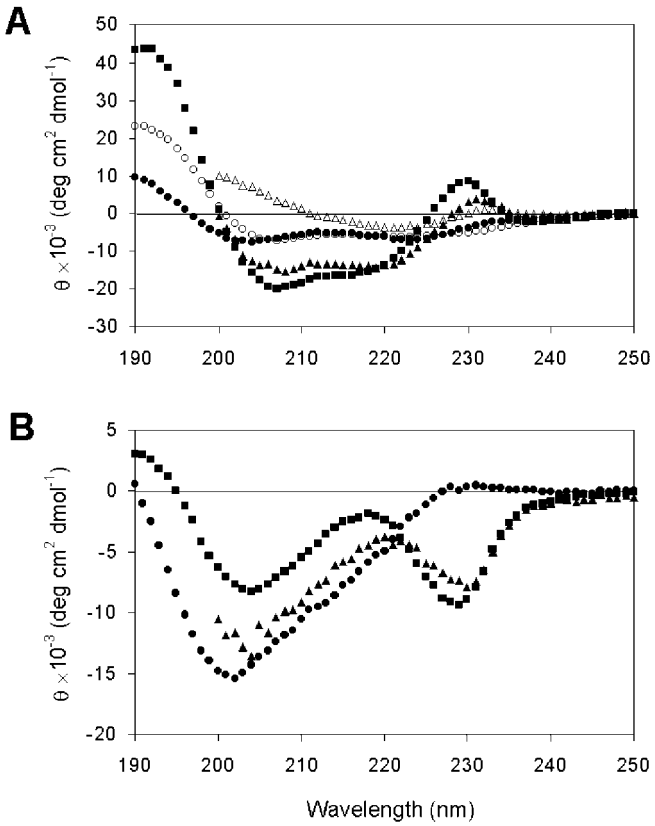

FIG. 5. **Circular dichroism spectra of CP10A (*A*) and indolicidin (*B*) in buffer (*closed circles*) and in complexes with POPC liposomes (*filled triangles*), POPG liposomes (*open triangles*), DPC (*squares*) and trifluoroethanol (*open circles*).** The spectrum of CP10A in the presence of POPC:POPG (7:3) liposomes was identical to that in POPC liposomes. The spectrum of indolicidin in the presence of POPG liposomes was identical to that in POPC liposomes. All samples contained 50 μM peptide in 10 mM sodium phosphate buffer (pH 7.0). The concentrations of lipid or detergent were 2 or 10 mM, respectively.

actions involving the five tryptophan side chains (6.9–7.5 ppm). The only overlap of backbone amide resonances occurred for Trp-8 H^N and Trp-9 H^N. However, at 42 °C these two resonances were resolved, allowing for the unambiguous assignment of the corresponding NOE cross-peaks. The sequential H^N-H^α contacts between the N-terminal four residues were stronger than the intra-residue H^N-H^α cross-peaks. Starting with residue 5 through to the C terminus, sequential H^N-H^α cross-peaks were weaker than intra-residue H^N-H^α contacts. Sequential H^N-H^N NOEs were mostly strong. Medium to weak H^α_i-H^N_{i+3} and H^α_i-H^β_{i+3} contacts were observed for residues 3–12 as well as one weak H^α_i-H^N_{i+4} contact connecting residues 8 and 12. This NOE cross-peak pattern is typical for a helical structure (37). Also present were weak H^α_i-H^N_{i+2} contacts between residues 3 and 13, which were slightly stronger toward the N terminus. These latter contacts are expected for a 3_{10} helix (37).

The structure of CP10A was calculated using 167 NOE-based distance restraints (77 intra-residue and 90 inter-residue restraints) using distance geometry-simulated annealing methods. On average, about 13 distance restraints per residue were applied, leading to a very well defined structure. The set of 15 calculated structures is shown in Fig. 7*A*. The structure was well defined between residues 4 and 13, with average pairwise root mean square deviations to the mean of 0.26 ± 0.05 Å for backbone atoms (N-C^α-C′) and 0.76 ± 0.17 Å for all heavy atoms. The dihedral angles for residues 5–12 were indicative of an α-helical structure, with the dihedral angles of residues 5 and 6 being closer to a 3_{10} helical conformation. The presence of hydrogen bonds was probed by the exchange of backbone amide protons against deuterium. Although no slow exchange, indicative of strong hydrogen bonds, was detected, the exchange for residues 8–12 was slower than for the N-terminal residues, indicating weak hydrogen bond formation. The backbone amide proton resonances of residues 8 or 9 and 11 were still observed in the one-dimensional spectrum 45 min after the addition of D_2O. No hydrogen bond restraints were applied during structure calculation. However, in the calculated structures, possible hydrogen bond partners were residues 4 and 5 for residue 8 and residues 7 and 8 for residue 11. The calculated structures also show hydrogen bonds between residues 6 and 10 as well as 8 and 12. Fig. 7*B* depicts the Schiffer-Edmundson helical wheel representation of CP10A. The molecule was amphipathic, with the positively charged lysine and arginine residues segregated on one side of the helix, forming a small hydrophilic face, whereas the tryptophan and alanine residues were mainly segregated on the other side of the helix, forming the large hydrophobic face.

DISCUSSION

The mesosomes seen in the electron micrographs are similar to those seen with other peptides including defensins (16), CP29, CP11CN, and Bac2A-NH_2 with *S. aureus* (14). Mesosomes have been proposed to be a fixation artifact that is indicative of some change or damage to the cytoplasmic membrane, although they also occur with the transcription inhibitor rifampin and the tetrahydrofolate reductase inhibitor trimethoprim (38). However, other peptides appeared to cause cell wall effects and abnormal septation as well as nuclear condensation with *S. epidermidis*, which was not observed for CP10A. Scanning electron micrographs of *S. epidermidis* treated with CP10A showed no significant difference in the outer surface of the bacteria compared with the control (data not shown). The varying effects of structurally diverse peptides led us to believe that different peptides may have a distinct mechanism of action that may include multiple targets (14). Here, CP10A appeared to have effects mainly on the interior of the bacterial cell. Macromolecular synthesis studies further verified that intracellular effects occurred even at sub-lethal peptide concentrations. Cessation of all macromolecular synthesis did not occur simultaneously, as would be expected if large cytoplasmic lesions occurred that resulted in loss of precursors or destruction of cellular ATP. Histidine and uridine incorporation appeared to be affected before thymidine incorporation. The MICs of peptides in the presence of LB and in the presence of synthetic media containing histidine, uridine, and thymidine were not significantly different, suggesting that the precursors were not acting as competitive inhibitors of the peptides. Therefore, the peptides did not interfere with precursor uptake into the cell and indeed affected macromolecular synthesis. It is thus likely that CP10A permeabilized the cytoplasmic membrane of *S. aureus* to reach an intracellular target.

The unique sequence and activity of CP10A made it an interesting candidate for structural analysis. The CD spectrum of CP10A in aqueous solution was not that of a random coil, in contrast to other α-helical cationic peptides studied, such as CEME and CEMA (39). This was unexpected for such a short peptide. However, upon interaction with lipids, the minima at 205 and 218 nm were greatly enhanced, indicating that there was a further induction of helical structure upon binding. In both lipids and detergent a maximum appeared at 230 nm. The latter was likely due to the contribution of ordered tryptophan side chains. Probably the minimum at 222 nm, expected for helical structure, was partially cancelled by the maximum at 230 nm. The shapes of the CD curves were similar in the

TABLE I
Proton Chemical Shifts of CP10A in DPC (molar ratio of peptide to DPC 1:100) at pH 4.0 and 37 °C

Residue	H^N	H^α	H^β	Other
Ile-1		3.88	1.99	H^γ 1.54, 1.19, 0.96 H^δ 0.88
Leu-2	8.77	4.29	1.62	H^γ 1.42 H^δ 0.91, 0.86
Ala-3	8.14	4.22	1.33	
Trp-4	7.98	4.45	3.24	H^ε1 10.43, H^δ1 7.34 H^ε3 7.39, H^ζ3 6.87 H^η2 7.03, H^ζ2 7.40
Lys-5	7.69	3.91	1.48	H^γ 0.88, H^δ 1.48 H^ε 2.74
Trp-6	7.63	4.56	3.36, 3.24	H^ε1 10.39, H^δ1 7.21 H^ε3 7.43, H^ζ3 6.69 H^η2 7.03, H^ζ2 7.43
Ala-7	7.93	4.05	1.41	
Trp-8	7.90	4.45	3.32, 3.24	H^ε1 10.28, H^δ1 7.06 H^ε3 7.48, H^ζ3 6.94 H^η2 7.14, H^ζ2 7.46
Trp-9	7.90	4.15	3.40, 3.31	H^ε1 10.36, H^δ1 7.19 H^ε3 7.44, H^ζ3 6.89 H^η2 7.11, H^ζ2 7.47
Ala-10	8.15	3.80	1.43	
Trp-11	8.09	4.27	3.30	H^ε1 10.39, H^δ1 6.94 H^ε3 7.36, H^ζ3 6.93 H^η2 7.08, H^ζ2 7.43
Arg-12	7.82	3.66	1.58, 1.51	H^γ 1.26, H^δ 2.77 H^ε 7.15, H^η 6.68
Arg-13	7.58	3.92	1.65, 1.53	H^γ 1.40, H^δ 2.81 H^ε 7.31, H^η 6.74 NH_2 7.47, 7.06

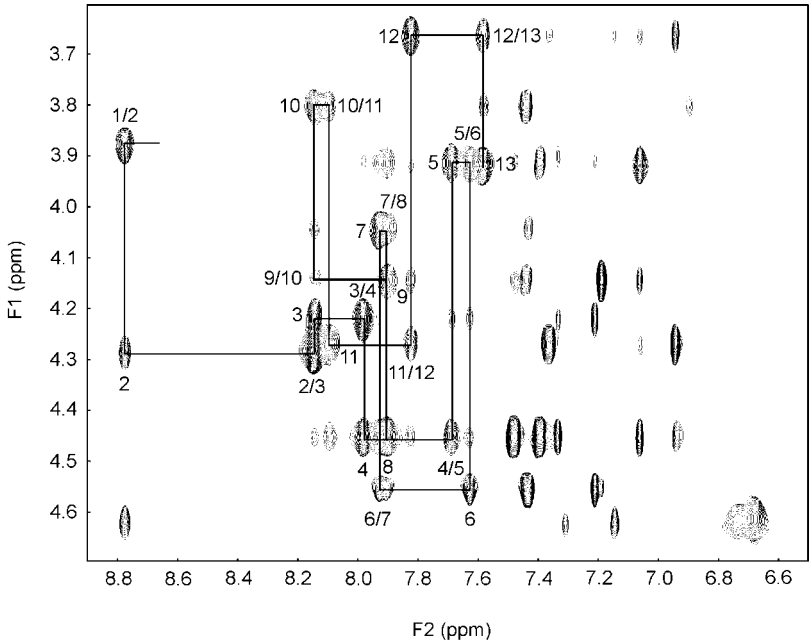

FIG. 6. **Portion of the NOESY spectrum (mixing time 70 ms) of CP10A at 37 °C and pH 4.0 showing the NOE cross-peaks between backbone α-protons with amide protons (7.5–8.8 ppm) as well as with tryptophan side-chain protons (6.9–7.5 ppm).** Sequential backbone assignments are labeled.

presence of POPC, mixed liposomes, and DPC, showing the same minima and maxima. The helix-inducing solvent trifluoroethanol was not able to promote the same content of α-helical structure that was seen with lipids. In addition, the maximum at 230 nm, due to the tryptophan contribution, was not present in trifluoroethanol. Apparently, the hydrophobic-hydrophilic interface provided by lipids is required for proper tryptophan orientation and helix formation. The blue shift of the fluorescence spectra in the presence of lipids indicated a movement of the tryptophan residues into a more hydrophobic environment. The small blue shift of 8 nm was consistent with experiments using membrane spin label probes, suggesting that the tryptophan residues on average were located in the relatively polar membrane interface. The tryptophan fluorescence of the peptide in lipid membranes was not quenched by the aqueous quencher KI, indicating that these residues became inaccessible to the buffer. The similar blue shift of CP10A in lipid vesicles and DPC suggested that the tryptophan residues in CP10A were in a similar environment. Furthermore, the tryptophan bands at 230 nm in the CD spectra were identical, indicating a similar orientation of tryptophan side chains with respect to the backbone.

The structure of CP10A in DPC micelles determined from NMR data was mainly α-helical with elements of 3_{10} helical geometry. Conformations close to the 3_{10} helix have been suggested to be transitional in the exchange between a random coil and helical conformations in peptides (40, 41). Since the CD spectra of CP10A in aqueous solution were not indicative of an

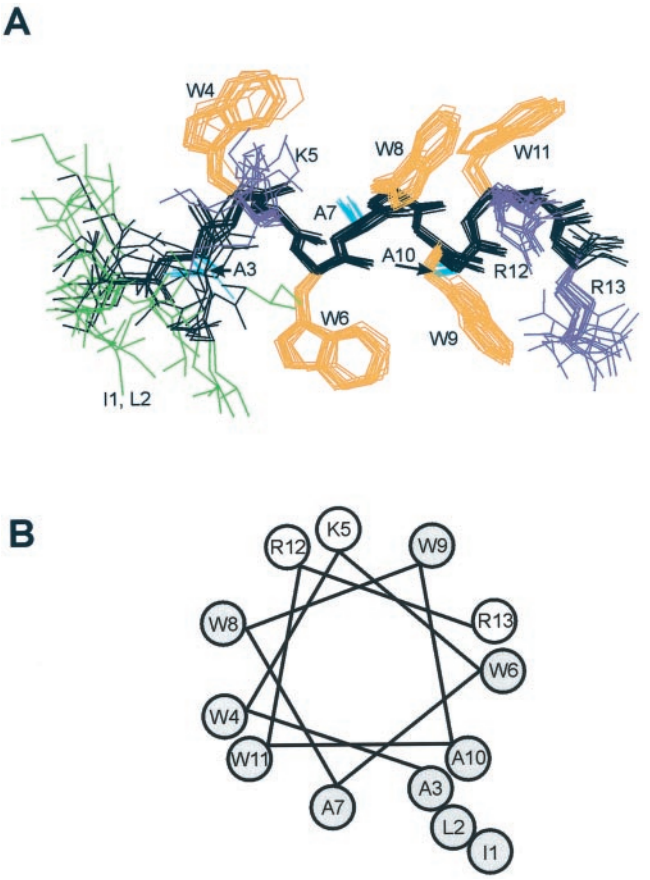

FIG. 7. *A*, a set of 15 structures calculated for CP10A. Shown are all heavy atoms superimposed over residues 4–13. The backbone atoms are colored *black*, whereas the side chain atoms are colored *green* (Ile-1, Leu-2), *blue* (alanine), *orange* (tryptophan), and *purple* (lysine and arginine). *B*, Schiffer-Edmundson helical wheel representation of CP10A residues 3–13. Residues Ile-1 and Leu-2 are not included because they are disordered. Hydrophobic residues are *shaded gray*.

unordered structure, the lipid-unbound and lipid-bound peptide may exchange between a 3_{10}-helical and an α-helical conformation, for which CD spectra are very similar. The structural differences between indolicidin (extended) and CP10A (helical) were brought about by the substitution of the three proline residues with alanine. Alanine has the largest helix-forming propensity of all natural amino acid residues, which has been attributed in part to its small side chain (42). The spacing of alanines in CP10A, three and four residues apart, may have had an additional helix-forming influence, since these small side chains lined up on the hydrophobic side of the peptide, thereby providing ample space for the bulky tryptophan side chains. Besides the formation of weak hydrogen bonds, the interaction of tryptophan side chains with the membrane interface likely has a major stabilizing influence on the structure of CP10A. Tryptophan was found to have the largest free energy of all natural amino acids (1.85 kcal/mol) for the partition between the aqueous phase and the membrane interface (43).

The C-terminal region, including the side chains of Arg-12 and Arg-13, of CP10A was unusually well defined. This stabilization could be due in part to backbone hydrogen bond formation with the amidated C terminus. Hydrogen bonds between residues 10 and 13 as well as between residue 11 and the C terminus were measured in the calculated structures but could not be confirmed by deuterium exchange experiments. The side chain of Arg-12 was oriented between the indole rings of Trp-8, Trp-9, and Trp-11, whereas the side chain of Arg-13 was oriented toward Trp-9 (Fig. 7*A*). This is consistent with the upfield shift of proton resonances for these residues due to aromatic ring current effects. Perhaps an interaction with the tryptophan indole rings stabilized the arginine side chain conformation. Arginine-aromatic interactions are a form of cation-π interactions and have been described as energetically favorable (44, 45). The tryptophan indole rings may partially shield the positively charged arginine side chains at the C-terminal end of CP10A and facilitate deeper embedding of the molecule into the membrane.

The profound change of structure in CP10A compared with indolicidin is likely responsible for its improved activity against Gram-positive bacteria. In fact, CP10A appeared to have properties that were reminiscent of other α-helical peptides rather than indolicidin. For instance, our data showed that CP10A was a much better membrane depolarizer than indolicidin (14). Furthermore, preliminary results indicated that CP10A induced lipid flip-flop similar to other helical peptides, whereas this was not observed for indolicidin. It is interesting to note, however, that good membrane depolarization by CP10A was not related to lysis of the bacterial membrane, as confirmed by our electron micrographs.

Conclusion—We have characterized a unique peptide, CP10A, using various biophysical and biochemical methods. Electron microscopy showed minimal effects of the peptide on the cell wall; however, membrane depolarization by CP10A was very efficient. Although no nuclear condensation was seen in the electron micrographs, macromolecular synthesis assays indicated that nucleic acid and protein production were affected by the peptide. We determined the structure and membrane location of CP10A using NMR, CD, and fluorescence spectroscopy. CP10A adopted a helical conformation in the presence of lipids, which was also present in aqueous solution. The location of CP10A was in the membrane interface, which is also the preferred location of the tryptophan indole ring. Cation-π interactions between the C-terminal arginine and tryptophan side chains contributed to peptide stability and may enhance membrane insertion. Taken together, our results describe a structure that seems to enable the peptide to cross the cell wall and cytoplasmic membrane of Gram-positive bacteria and suppress intracellular processes. Our findings support a growing body of evidence that antimicrobial peptides may not solely kill by membrane disruption but may follow various mechanisms of action, including intracellular targets. The structure of CP10A may thus serve as a template for the design of future therapeutics.

Acknowledgments—We thank Dr. Lawrence P. McIntosh (Protein Engineering Network of Centers of Excellence and Departments of Chemistry, Biochemistry, and Molecular Biology, University of British Columbia, Vancouver BC, Canada) and Dr. Robert J. Cushley (Institute of Molecular Biology and Biochemistry and Department of Chemistry, Simon Fraser University, Burnaby BC, Canada) for assistance in the acquisition of NMR spectra.

REFERENCES

1. Hancock, R. E. W., Falla, T. J., and Brown, M. (1995) *Adv. Microb. Physiol.* **37,** 136–175
2. Piers, K. L., and Hancock, R. E. W. (1994) *Mol. Microbiol.* **12,** 951–958
3. Sawyer, J. G., Martin, N. L., and Hancock, R. E. (1988) *Infect. Immun.* **56,** 693–698
4. Peterson, A. A., Fesik, S. W., and McGroarty, E. J. (1987) *Antimicrob. Agents Chemother.* **31,** 230–237
5. Lehrer, R. I., Barton, A., Daher, K. A., Harwig, S. S., Ganz, T., and Selsted, M. E. (1989) *J. Clin. Invest.* **84,** 553–561
6. Cociancich, S., Ghazi, A., Hoffman, J. A., Hetrus, C., and Letellier, C. (1993) *J. Biol. Chem.* **268,** 19239–19245
7. Juretic, D., Chan, H. C., Brown, J. H., Morell, J. L., Hendler, R. W., and Westerhoff, H. (1989) *FEBS Lett.* **249,** 219–223
8. Wu, M., Maier, E., Benz, R., and Hancock, R. E. W. (1999) *Biochemistry* **38,** 7235–7242
9. Park, C. B., Kim, H. S., and Kim, S. C. (1998) *Biochem. Biophys. Res. Commun.* **244,** 253–257
10. Zhang, L., Benz, R., and Hancock, R. E. W. (1999) *Biochemistry* **38,** 8102–8111

11. Selsted, M. E., Novotny, M. J., Morris, W. L., Tang, Y. Q., Smith, W., and Cullor, J. S. (1992) *J. Biol. Chem.* **267,** 4292–4295
12. Rozek, A., Friedrich, C. L., and Hancock, R. E. W. (2000) *Biochemistry* **39,** 15765–15774
13. Subbalakshmi, C., Krishnakumari, V., Nagaraj, R., and Sitaram, N. (1996) *FEBS Lett.* **395,** 48–52
14. Friedrich, C. L., Moyles, D., Beveridge, T. J., and Hancock, R. E. W. (2000) *Antimicrob. Agents Chemother.* **44,** 2086–2092
15. Yeaman, M. R., Bayer, A. S., Koo, S. P., Foss, W., and Sullam, P. M. (1998) *J. Clin. Invest.* **101,** 178–187
16. Shimoda, M., Ohki, K., Shimamoto, Y., and Kohashi, O. (1995) *Infect. Immun.* **63,** 2886–2891
17. Xiong, Y. Q., Yeaman, M. R., and Bayer, A. S. (1999) *Antimicrob. Agents Chemother.* **43,** 1111–1117
18. Scott, M. G., Gold, M. R., and Hancock, R. E. W. (1999) *Infect. Immun.* **67,** 6445–6453
19. Amsterdam, D. (1996) in *Antibiotics in Laboratory Medicine* (Lorian, V., ed) 4th Ed., pp. 52–111, Lippincott Williams & Wilkins, Baltimore
20. Sims, P. J., Waggoner, A. S., Wang, C. H., and Hoffman, J. F. (1974) *Biochemistry* **13,** 3315–3330
21. Braunschweiler, L., and Ernst, R. R. (1983) *J. Magn. Res.* **53,** 521–528
22. Jeener, J., Meier, B. H., Bachmann, P., and Ernst, R. R. (1979) *J. Chem. Phys.* **71,** 4546–4553
23. Rance, M., Sørensen, O. W., Bodenhausen, G., Wagner, G., Ernst, R. R., and Wüthrich, K. (1983) *Biochem. Biophys. Res. Commun.* **117,** 479–485
24. Piotto, M., Saudek, V., and Sklenar, V. (1992) *J. Biomol. NMR* **2,** 661–665
25. Sklenar, V., Piotto, M., Leppik, R., and Saudek, V. (1993) *J. Magn. Res. A* **102,** 241–245
26. Bax, A., and Davis, D. G. (1985) *J. Magn. Res.* **65,** 355–360
27. Delaglio, F., Grzesiek, S., Vuister, G. W., Zhu, G., Pfeifer, J., and Bax, A. (1995) *J. Biomol. NMR* **6,** 277–293
28. Johnson, B. A., and Blevins, R. A. (1994) *J. Biomol. NMR* **4,** 603–614
29. Hyberts, S. G., Goldberg, M. S., Havel, T. F., and Wagner, G. (1992) *Protein Sci.* **1,** 736–751
30. Kuszewski, J., Nilges, M., and Brunger, A. T. (1992) *J. Biomol. NMR* **2,** 33–56
31. Nilges, M., Clore, G. M., and Gronenborn, A. M. (1988) *FEBS Lett.* **229,** 317–324
32. Nilges, M., Kuszewski, J., and Brunger, A. T. (1991) in *Computational Aspects of the Study of Biological Macromolecules by NMR* (Hoch, J. C., ed) Plenum Press, New York
33. Lakowicz, J. R. (1983) *Principles of Fluorescence Spectroscopy*, Plenum Press, New York
34. Wallace, B. A., and Mao, D. (1984) *Anal. Biochem.* **142,** 317–328
35. Holzwarth, G. M., and Doty, P. (1965) *J. Am. Chem. Soc.* **87,** 218–228
36. Woody, R. W. (1994) *Eur. Biophys. J.* **23,** 253–262
37. Wüthrich, K. (1986) *NMR of Proteins and Nucleic Acids*, John Wiley & Sons, Inc., New York
38. Beveridge, T. J. (1989) in *Bacteria in Nature: A Treatise on the Interaction of Bacteria and Their Habitats* (Leadbetter, E. R., and Poindexter, J. S., eds) Vol. 3, pp. 1–65, Plenum Publishing Corp., New York
39. Friedrich, C., Scott, M. G., Karunaratne, N., Yan, H., and Hancock, R. E. (1999) *Antimicrob. Agents. Chemother.* **43,** 1542–1548
40. Huo, S., and Straub, J. E. (1999) *Proteins* **36,** 249–261
41. Millhauser, G. L. (1995) *Biochemistry* **34,** 3873–3877
42. Chakrabartty, A., Kortemme, T., and Baldwin, R. L. (1994) *Protein Sci.* **3,** 843–852
43. Wimley, W. C., and White, S. H. (1996) *Nat. Struct. Biol.* **3,** 842–848
44. Dougherty, D. A. (1996) *Science* **271,** 163–168
45. Flocco, M. M., and Mowbray, S. L. (1994) *J. Mol. Biol.* **235,** 709–717